Gallic acid enhances pirarubicin-induced anticancer in living K562 and K562/Dox leukemia cancer cells through cellular energetic state impairment and P-glycoprotein inhibition

KHIN THENU AYE[1-3], SAKORNNIYA WATTANAPONGPITAK[1,2], BENJAMAPORN SUPAWAT[1,2], SUCHART KOTHAN[1,2], CHATCHANOK UDOMTANAKUNCHAI[1,2], SINGKOME TIMA[4], JIE PAN[2,5] and MONTREE TUNGJAI[1,2]

[1]Department of Radiologic Technology, Faculty of Associated Medical Sciences, Chiang Mai University; [2]Center of Radiation Research and Medical Imaging, Department of Radiologic Technology, Faculty of Associated Medical Sciences, Chiang Mai University; [3]Ph.D. Degree Program in Biomedical Sciences, Faculty of Associated Medical Sciences, Chiang Mai University, Under The CMU Presidential Scholarship; [4]Department of Medical Technology, Faculty of Associated Medical Sciences, Chiang Mai University, Chiang Mai 50200, Thailand; [5]Shandong Provincial Key Laboratory of Animal Resistant Biology, College of Life Sciences, Shandong Normal University, Jinan, Shandong 250014, P.R. China

Received December 28, 2020; Accepted July 22, 2021

DOI: 10.3892/or.2021.8178

Abstract. Leukemia is a common malignancy affecting humans worldwide. Pirarubicin (Pira) is one of the anticancer agents used for the treatment of leukemia. Although Pira is effective, drug resistance may develop in cancer cells exposed to this drug, whereas the combination of natural products with Pira may help to overcome this problem. The aim of the present study was to focus on the effect of gallic acid (GA) on the anticancer activity of Pira in K562 leukemia cells and K562/doxorubicin (Dox)-resistant leukemia cells in order to investigate the possible underlying mechanisms. The cell viability, mitochondrial activity, mitochondrial membrane potential ($\Delta\Psi m$) and ATP levels were assessed in living K562 and K562/Dox cancer cells following treatment with GA/Pira combination, GA alone or Pira alone. P-glycoprotein-mediated efflux of Pira was determined in GA-treated K562/Dox cancer cells. The results demonstrated that GA/Pira combination decreased cell viability, mitochondrial activity, $\Delta\Psi m$ and ATP levels in K562 and K562/Dox cancer cells in a GA concentration-dependent manner compared with non-treated or Pira-treated cells. GA inhibited P-glycoprotein-mediated efflux of Pira in GA-treated K562/Dox cancer cells. Therefore, GA enhanced the anticancer effect of Pira on K562 and K562/Dox cancer cells through cellular energy status impairment, and was able to reverse drug resistance in living K562/Dox cancer cells by inhibiting the function of P-glycoprotein.

Correspondence to: Dr Montree Tungjai, Department of Radiologic Technology, Faculty of Associated Medical Sciences, Chiang Mai University, 110 Intawaroros Road, Sripoom, Chiang Mai 50200, Thailand
E-mail: mtungjai@gmail.com

Key words: gallic acid, multidrug resistance, P-glycoprotein, pirarubicin, cancer

Introduction

Cancer is a major cause of morbidity and mortality worldwide. Several types of malignant diseases have been characterized to date. Leukemia, which is a term used to describe a group of hematological malignancies, is one of the major causes of cancer-related mortality globally (1). Treatment of leukemia with chemotherapy is a common approach. Anthracyclines and their derivatives, including doxorubicin (Dox), are anticancer drugs commonly used as chemotherapy for hematological malignancies in the clinical setting (2-4). Pirarubicin (Pira) is a Dox derivative that exhibits higher toxicity compared with Dox against cancer cells, but has been associated with lower cardiotoxicity than Dox in hamsters (5-7). Pira is used for the treatment of several malignancies, such as head and neck cancer, ovarian cancer, lymphoma and leukemia (8). There is evidence indicating that anthracyclines induce reactive oxygen species (ROS) generation, resulting in DNA damage (2-4). Mizutani *et al* (8) investigated the mechanisms of action of Pira in the induction of apoptosis via ROS generation, and revealed that Pira induced hydrogen peroxide (H_2O_2) generation and apoptosis of both HL-60 and HL-100 cells. The authors suggested that Pira induced cell apoptosis through H_2O_2 generation.

However, chemotherapy with anthracycline drugs for leukemia is often limited by the development of multidrug resistance (MDR) in cancer cells (9,10). MDR is observed when cells exhibit simultaneous resistance to various drugs without similar chemical structure and with different cellular

targets. The mechanism identified by these MDR studies is considered to involve P-glycoprotein-mediated efflux of anticancer drugs. P-glycoprotein is an ATP-dependent plasma membrane protein (11-13). Certain compounds have exhibited the ability to reverse MDR in cancer cells, resulting in intracellular accumulation of anticancer drugs and making them a good choice for MDR cancer treatment; however, these MDR-reversing agents, such as cyclosporin A, verapamil, reserpine, quinidine and tamoxifen, are associated with unwanted side effects (13,14). Therefore, finding a new approach to overcoming MDR in cancer cells that includes MDR-reversing agents without unwanted side effects poses a challenge.

Several studies have reported the potential anticancer effects of natural products on various cancer cells (15-19). Gallic acid (GA) is a 3,4,5-trihydroxybenzoic acid that is distributed in various natural products (20,21). GA has exhibited anticancer activity without damage to normal cells (22-26). Based on that evidence on the effects of GA on cancerous and normal cells, it appears that GA may hold promise for overcoming MDR of cancer cells. In addition, it was hypothesized that GA may help to enhance the anticancer activity of Pira in MDR cancer cells. However, GA has been revealed to have strong antioxidant activity (27-29), which may also affect the effectiveness of cancer treatment by Pira, as Pira-induced cell death occurs via ROS generation. Therefore, these findings raised the question of whether GA (which has antioxidant properties) could modify the cytotoxicity of Pira (which has pro-oxidant properties) in cancer cells. The present study was undertaken to investigate the effect of GA on the anticancer activity of Pira in K562 and K562/Dox MDR leukemia cells and elucidate the potential underlying mechanisms.

Materials and methods

Chemicals. Pira (product no. P8624; Fig. 1A), GA (product no. 398225; Fig. 1B), rhodamine B (product no. 83689), MTT (product no. M2003) and resazurin (product no. R7017) were purchased from Sigma-Aldrich; Merck KGaA. FBS (cat. no. FBS-11A) and penicillin/streptomycin (cat. no. PS-B) were purchased from Capricorn Scientific. RPMI-1640 medium (product no. RPP10) was purchased from Caisson Labs.

Cell lines and cell culture. The K562 human leukemia cell line and its Dox-resistant counterpart, K562/Dox (P-glycoprotein-overexpressing cells) were provided by author CU. The cells were cultured in RPMI-1640 medium supplemented with 10% heat-inactivated FBS and 1% penicillin/streptomycin in a humidified atmosphere with 5% CO_2 at 37˚C. The initial cell density was $1x10^5$ cells/ml and reached 8-$10x10^5$ cells/ml 72 h later. Cells were routinely sub-cultured at 72 h.

For the experiments, the initial cell density was $5x10^5$ cells/ml and reached 8-$10x10^5$ cells/ml 24 h later. Cells were found to be at the exponential growth phase.

Cytotoxic assay. Cytotoxicity was assessed using the resazurin assay as previously described (30). Cells ($5x10^4$ cells/ml) were incubated with various concentrations of GA (0, 0.1, 1, 10, 100 and 200 μM) or Pira (0, 1, 10, 100, 300 and 500 nM) in complete RPMI-1640 medium and placed into a humidified atmosphere with 5% CO_2 at 37˚C for 48 and 72 h. Subsequently, 100 μl resazurin (blue and non-fluorescent dye, 0.1 mg/ml) was added to the system. After 4 h, red fluorescent dye resorufin was obtained. The fluorescence emission at 590 nm and excitation wavelength at 570 nm were assessed by a spectrofluorometer (LS55; Perkin Elmer, Inc.). Of note, there were several *in vitro* studies on anticancer activities of GA which used concentrations of GA ranging from 10-500 μM (31-37).

Co-treatment. Cells ($5x10^4$ cells/ml) were incubated with 10 or 100 μM GA and 10 nM Pira in complete RPMI-1640 medium in a humidified atmosphere with 5% CO_2 at 37˚C for 48 and 72 h. Next, 100 μl resazurin (0.1 mg/ml) was added to the system. After 4 h, red fluorescent dye resorufin was obtained. The fluorescence emission at 590 nm and excitation wavelength at 570 nm were assessed by a spectrofluorometer (LS55; Perkin Elmer, Inc.).

Synergism quotient (SQ) calculation. The SQ was calculated by subtracting baseline values from all treatments, then dividing the net effect of the combination drugs (GA/Pira) by the sum of individual effects of drugs (GA + Pira). SQ >1.0 indicated a synergistic effect.

Mitochondrial activity determination. The mitochondrial activity was determined by MTT-reduction assay. The solvent used to dissolve the purple formazan was dimethyl sulfoxide (DMSO). Mitochondrial reductase reduced MTT, a yellow tetrazole, to purple formazan in living cells. Cells ($5x10^4$ cells/ml) were incubated with GA (10 and 100 μM) or Pira (10 nM) or GA/Pira combination (10/10 and 100 μM/10 nM) in complete RPMI-1640 medium in a humidified atmosphere with 5% CO_2 at 37˚C for 3 h. Next, 200 μM MTT was added to the system. After 20 min, purple formazan was obtained. The absorption intensity at 560 nm was measured by the UV-visible spectrophotometer (Agilent Technologies, Inc.).

Mitochondrial membrane potential ($\Delta\Psi$m) measurement. The $\Delta\Psi$m was measured by using the non-invasive functional spectrofluorometric method previously described (38-40). Briefly, $2x10^6$ cells/ml were incubated with GA (10 and 100 μM) or Pira (10 nM) or GA/Pira combination (10/10 and 100 μM/10 nM) for 3 h and were then suspended with 40 nM rhodamine B in 2 ml HEPES-Na^+ buffer (pH 7.25) and vigorously stirred at 37˚C. The fluorescence spectrum of rhodamine B (emission wavelength at 582 nm and excitation wavelength at 553 nm) was recorded as a function of time. Next, 200 μM MTT was added to the system after cells had been incubated with rhodamine B for 20 min, resulting in a progressive decrease in rhodamine B fluorescence. $\Delta\Psi$m was calculated by the following equation: $\Delta\Psi$=-61.51 logVi-258.46 mV, where Vi=initial rate of decrease in rhodamine B fluorescence=(dF/dt) x (C_T/F_0), nM/sec. dF/dt=slope of the tangent to the curve F=f(t) after the addition of MTT. C_T=rhodamine B concentration, F_0=rhodamine B fluorescence intensity. In the present study, $\Delta\Psi$m values are presented as an absolute |$\Delta\Psi$m| value.

ATP measurement. Cellular ATP was extracted by the single-step ATP extraction method using boiling water as previously described (41). Briefly, $2x10^6$ cells/ml were

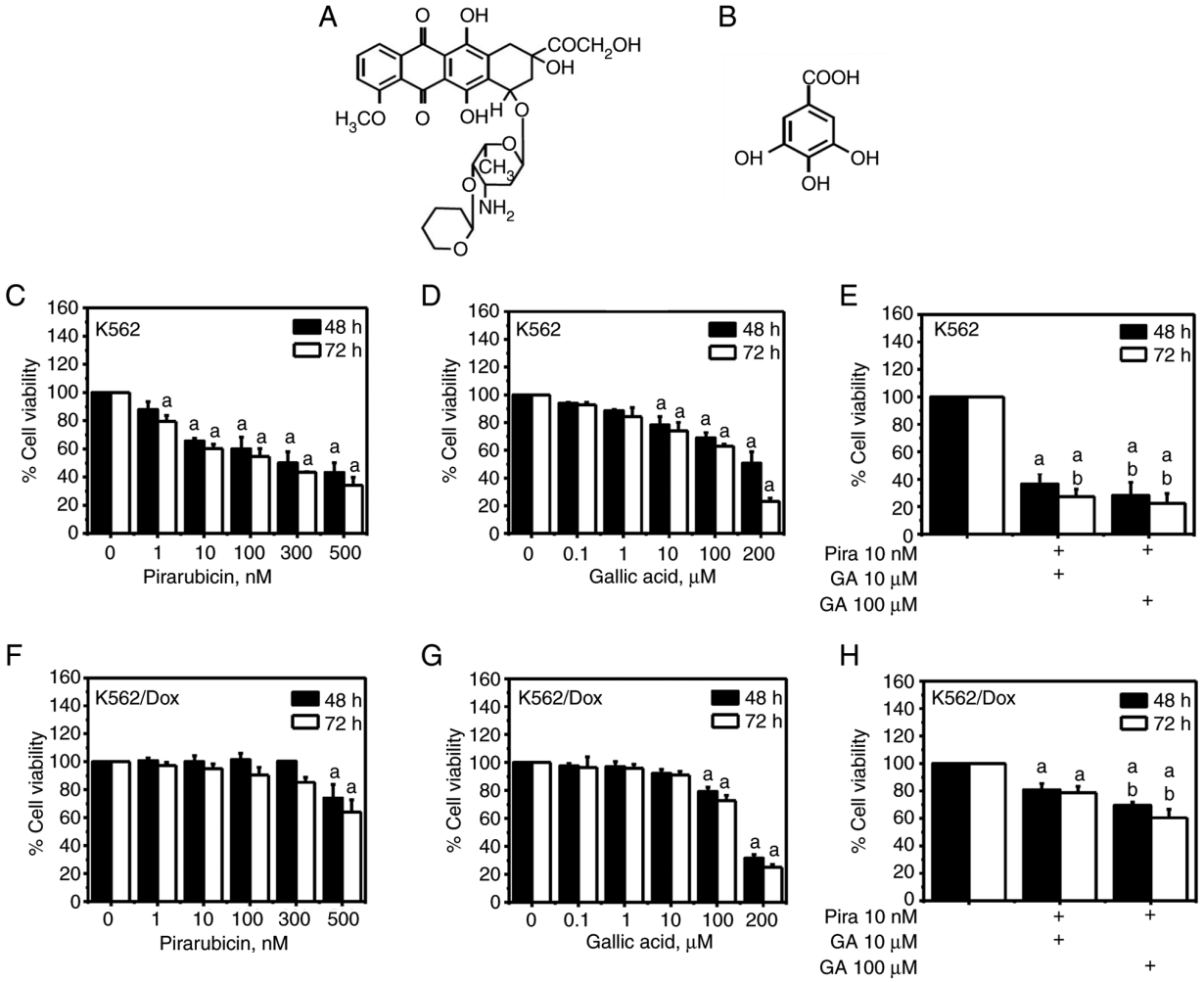

Figure 1. Chemical structure of (A) Pira and (B) GA. Effect of Pira on (C) K562 and (F) K562/Dox cancer cell viability. Effect of GA on (D) K562 and (G) K562/Dox cancer cell viability. Effect of GA/Pira combination on (E) K562 and (H) K562/Dox cancer cell viability. Treatment times: ▬48 and ▭72 h. [a]P<0.05 when compared with control and [b]P<0.05 when compared with 10 nM Pira. Pira, pirarubicin; GA, gallic acid; Dox, doxorubicin.

incubated with GA or Pira or GA/Pira combination in 2 ml HEPES-Na^+ buffer (pH 7.25) at 37˚C for 3 h. The cells were centrifuged at 2,000 x g for 1 min and then cell pellets were collected. Cellular ATP was extracted by adding 1 ml boiling water (60˚C) to the cell pellets, followed by vortexing and centrifugation at 2,000 x g for 1 min, room temperature. The supernatant was used for ATP measurement. The supernatant was purified by thin-layer chromatography (TLC). The stationary phase was silica-coated aluminum (TLC silica gel 60 F254; Merck KGaA). The mobile phase consisted of butanol:acetic acid:water at a ratio of 4:1:5 (v/v). ATP standard was used as a reference. The retardation factor was 0 for the ATP standard when applied to the stationary and mobile phases. Purified ATP samples were measured by spectrofluorometry. The fluorescence spectrum of purified ATP samples was recorded at a fluorescence emission range of 390-500 nm, with an emission peak at 410 nm (excitation at 360 nm).

Determination of P-glycoprotein function in living K562/Dox cancer cells. The P-glycoprotein function in living K562/Dox cancer cells was assessed using a non-invasive functional spectrofluorometric method (LS55; Perkin Elmer, Inc.) as previously described (40,42). Briefly, $2x10^6$ cells/ml were suspended in 2 ml HEPES-Na^+ buffer (pH 7.25) at 37˚C and were continually stirred using a 1-cm quartz cuvette (Hellma Analytics). Pira (1 μM) was added to the system. The fluorescence intensity of Pira at 590 nm (excitation at 480 nm) was recorded as a function of time. At the steady state, GA at various concentrations (0, 10, 50, 100 and 200 μM) was added. Subsequently, 5 μl of 4% Triton X-100 solution was added, resulting in the system entering the equilibrium state.

In the present study, the P-glycoprotein function is presented as P-glycoprotein-mediated active efflux coefficient (k_a). The ability of GA to inhibit the function of P-glycoprotein was determined using the following ratio: k_a^i/k_a^0 where k_a^i=P-glycoprotein-mediated active efflux of Pira in the presence of GA; and k_a^0=P-glycoprotein-mediated active efflux of Pira in the absence of GA. When k_a^i/k_a^0=1, GA cannot inhibit active efflux. When k_a^i/k_a^0=0, GA can completely inhibit active efflux.

The overall concentration of Pira accumulation in cells (C_n) and concentration of Pira accumulation in the cytoplasm (C_i) were also determined.

Resistance factor (RF) calculation. RF in drug-resistant cells with P-glycoprotein expression contributed to the kinetics

of passive and active efflux of Pira, which was previously described (43). RF could theoretically be calculated as follows: $RF=1 + k_a/k_+$ where k_+=passive influx coefficient; and k_a=P-glycoprotein-mediated active efflux coefficient.

Intracellular pH (pH_i) measurements. In order to analyze the kinetics of Pira transport into the cells, the free Pira concentration in the cytoplasm may be calculated as previously described (44): $C_i=C_e (1+10^{pKa-pHi})/(1+10^{pKa-pHe})$, which may be re-written as follows: $pH_i=pK_a-\log [C_i (1+10^{pKa-pHe})]/C_e$ where C_i=intracellular free Pira concentration in the steady state, C_e=extracellular free Pira concentration in the steady state, pK_a=7.7 for Pira, pH_e=7.25 at 37˚C

Statistical analysis. Statistical analysis was performed using Microsoft Excel 2010 (Microsoft Corporation) and OriginPro 2015 (OriginLab Corporation). The number of repeats was 5. The data in the present study are expressed as the mean ± standard error of the mean (SEM). To evaluate statistical differences in the mean values between each treated group and the non-treated control group, one-way ANOVA was used to assess the significance of GA concentration. The post hoc test (Tukey's test) was used to evaluate statistical differences in the mean values between each group. $P<0.05$ was considered to indicate a statistically significant difference.

Results

Effect of GA and Pira on K562 and K562/Dox cancer cell viability. Fig. 1C, D, F and G revealed the effects of Pira and GA on K562 (Fig. 1C and D) and K562/Dox (Fig. 1F and G) cancer cell viability at 48 and 72 h. These results demonstrated that Pira and GA decreased K562 cancer cell viability in a dose- and time-dependent manner. The viability of K562/Dox cancer cells in the presence of GA (0.1, 1 and 10 μM) and Pira (1, 10, 100 and 300 nM) did not significantly change at 48 and 72 h compared with the control group. High concentrations of GA (100 and 200 μM) were associated with a change in cell viability to 79 and 31% at 48 h, and to 72 and 25% at 72 h, respectively. Treatment with 500 μM Pira was associated with a change in cell viability to 73% at 48 h and 64% at 72 h.

The results indicated that GA and Pira decreased the viability of K562 and K562/Dox cancer cells in a concentration- and treatment time-dependent manner.

Effect of GA/Pira combination on K562 and K562/Dox cancer cell viability. The data demonstrated that 10 nM Pira significantly decreased the viability of K562 cancer cells at 48 and 72 h to 65 and 60% (Fig. 1C), respectively, and decreased the viability of K562/Dox cancer cells at 72 h to 95% (Fig. 1F), compared with the control group. The viability of K562/Dox cancer cells treated with 10 nM Pira did not change at 48 h. Fig. 1E and H revealed the percentage (%) of cell viability in treated (with a combination of Pira and GA) K562 and K562/Dox cancer cells and non-treated cells at 48 and 72 h.

In the GA/Pira combination group, the viability of K562 cancer cells decreased following treatment with a combination of 10 nM Pira with 10 or 100 μM GA, specifically to 36 or 28% at 48 h and to 27 or 22% at 72 h, respectively, compared with the control group (Fig. 1E). The viability of K562/Dox cancer cells decreased following treatment with a combination of 10 nM Pira and 10 or 100 μM GA, specifically to 80 or 69% at 48 h and to 78 or 60% at 72 h, respectively, compared with the control group (Fig. 1H).

Table I. SQ calculation.

	SQ values			
	K562 cancer cells		K562/Dox cancer cells	
Combinations	48 h	72 h	48 h	72 h
Pira 10 nM/GA10 μM	1.13	1.10	2.42	1.54
Pira 10 nM/GA 100 μM	1.10	1.01	1.47	1.23

SQ, synergism quotient; Pira, pirarubicin; GA, gallic acid; Dox, doxorubicin.

In addition, as revealed in Table I, the SQ calculation of cell viability (48 and 72 h) indicated a synergistic effect of the GA/Pira combination. These results indicated that GA enhanced the cytotoxic effect of Pira on both K562 and K562/Dox cancer cells in a concentration- and treatment time-dependent manner.

The microscopic examination revealed rough, shrinking, irregularly shaped cells, and decreases in cell density as shown in Fig. 2. These findings were linked to cell death. Of note, the present study used higher concentrations of Pira and GA in Fig. 2 because there were clearly observable cell morphological changes.

Effect of GA/Pira combination on mitochondrial activity in K562 and K562/Dox cancer cells. The mitochondrial activity was determined by the reduction of MTT to insoluble purple formazan. The reaction was followed by the alteration of absorbance intensity at 560 nm. Therefore, increments of absorbance intensity at 560 nm were considered as an indication of increased mitochondrial activity. Fig. 3A and B revealed the alterations in absorbance intensity at 560 nm of treated K562 and K562/Dox cancer cells and non-treated cells. The absorbance intensity at 560 nm was decreased in K562 and K562/Dox cancer cells treated with 10 nM Pira and 10 or 100 μM GA compared with the control group.

In the GA/Pira combination group, absorbance intensity at 560 nm was decreased in K562 cancer cells treated with a combination of 10 nM Pira and 10 or 100 μM GA, as it changed to 81 or 72%, respectively, compared with the control group (Fig. 3A). The absorbance intensity at 560 nm was decreased in K562/Dox cancer cells treated with a combination of 10 nM Pira and 10 or 100 μM GA, specifically changing to 72 or 70% compared with the control group ($P<0.05$), and to 82 or 80% compared with the 10-nM Pira alone group, respectively (Fig. 3B).

These results indicated that GA significantly enhanced the Pira-induced mitochondrial activity that was decreased in K562/Dox cancer cells. Moreover, GA enhanced the Pira-induced mitochondrial activity that was decreased in K562 cancer cells, but the difference was not statistically significant.

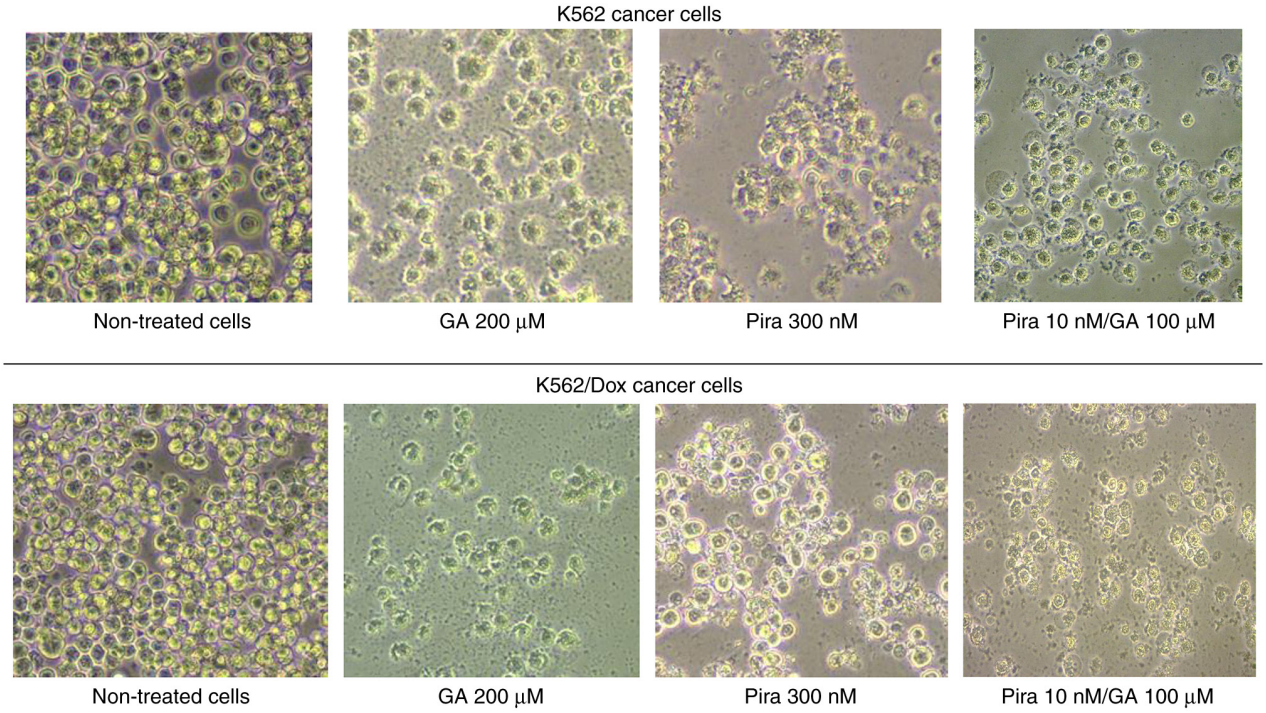

Figure 2. Microscopic images (magnification, x100) of treated K562 and K562/Dox cancer cells and non-treated cells at 72 h. Pira, pirarubicin; GA, gallic acid; Dox, doxorubicin.

Effect of GA/Pira combination on the |ΔΨm| of K562 and K562/Dox cancer cells. Fig. 3C and D revealed the effect of GA/Pira combination on |ΔΨm| of K562 and K562/Dox cancer cells. This data demonstrated that 10 nM Pira decreased the |ΔΨm| of K562 and K562/Dox cells by 5% compared with the control group, whereas 10 or 100 μM GA decreased the |ΔΨm| by 10 or 14% and by 4 or 8% for K562 and K562/Dox cancer cells respectively, compared with the control group.

In the GA/Pira combination group, the |ΔΨm| of K562 cancer cells significantly decreased with the combination of 10 nM Pira with 10 or 100 μM GA, specifically changing to 83 or 82% compared with the control group, and to 87 or 86% compared with the 10 nM Pira alone group, respectively (Fig. 3C). The |ΔΨm| of K562/Dox cancer cells decreased following treatment with the combination of 10 nM Pira with 10 or 100 μM GA, specifically changing to 87 or 86% compared with the control group ($P<0.05$) and to 92 or 90% compared with the 10 nM Pira alone group, respectively (Fig. 3D).

These results indicated that GA enhanced the Pira-induced ΔΨm disruption in both K562 and K562/Dox cancer cells in a concentration-dependent manner.

Effect of GA/Pira on ATP levels in K562 and K562/Dox cancer cells. The ATP level was assessed by determining the fluorescence emission intensity at 410 nm. Subsequently, the changes in fluorescence emission intensity in treated cell groups were compared with the control group. The change in intensity was considered to reflect ATP level changes and the minus symbol indicates decrement. Fig. 3E and F revealed the percentage (%) of change of ATP levels in treated K562 and treated K562/Dox cancer cells and non-treated cells. The percentage (%) of decrease in ATP levels was observed in K562 and K562/Dox cancer cells treated with 10 nM Pira and 10 or 100 μM GA compared with the control group.

In the GA/Pira combination group, the percentage (%) of decrease in ATP levels was significant in K562 cancer cells treated with a combination of 10 nM Pira and 10 or 100 μM GA compared with the control group (Fig. 3E). The percentage (%) of decrease in ATP levels was significant in K562/Dox cancer cells treated with a combination of 10 nM Pira and 10 or 100 μM GA compared with the control group (Fig. 3F).

These results indicated that GA enhanced the Pira-induced decrease in ATP levels in both K562 and K562/Dox cancer cells in a concentration-dependent manner.

Effect of GA on P-glycoprotein function in K562/Dox cancer cells. The kinetic parameters of Pira uptake into GA-treated K562 and GA-treated K562/Dox cancer cells and non-treated cells are revealed in Table II. The V_+ and k_+ values were significantly decreased in K562 cancer cells following treatment with 50, 100 and 200 μM GA, whereas these two values did not significantly change in GA-treated K562/Dox cancer cells compared with the control group. However, V_a and k_a values were decreased in K562/Dox cancer cells.

The C_n and C_i values were increased in K562/Dox cancer cells treated with 50, 100 and 200 μM GA, whereas these values did not change in GA-treated K562 cancer cells at all GA concentrations compared with the control group (Fig. 4A and B). Fig. 4C revealed the ratio of k_a^i/k_a^0 values in GA-treated K562/Dox cancer cells. The data revealed decreases in the k_a^i/k_a^0 ratio values in GA-treated K562/Dox cancer cells at 50, 100 and 200 μM GA.

These data indicated that GA inhibited P-glycoprotein from pumping Pira out of the cells, resulting in increased intracellular Pira accumulation.

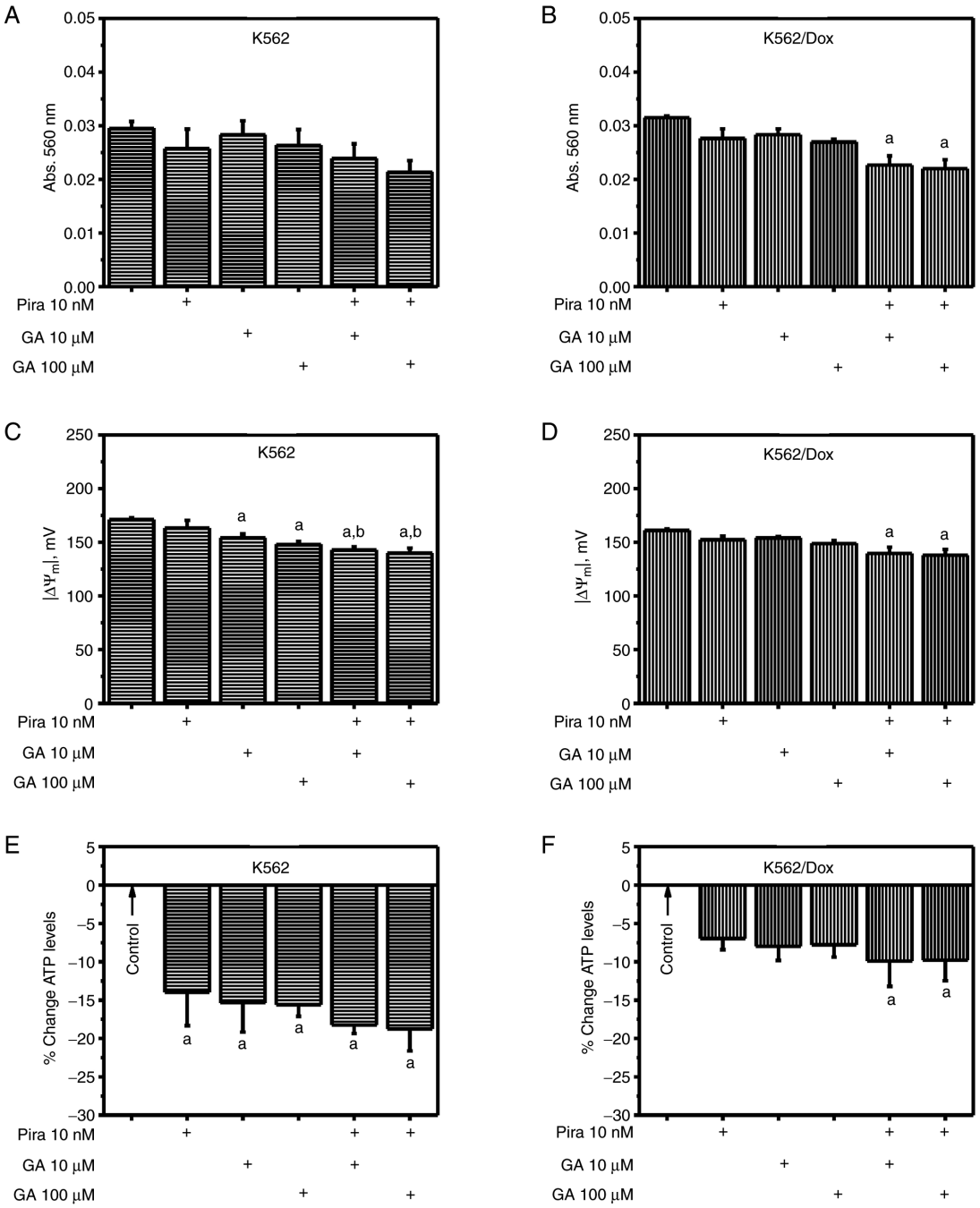

Figure 3. Effect of Pira, GA and Pira/GA on mitochondrial activity, ΔΨm and ATP levels in K562 and K562/Dox cancer cells. Abs at 560 nm of (A) treated K562 and (B) treated K562/Dox cancer cells and non-treated cells. The abs at 560 nm decreased, reflecting a decrease in the mitochondrial activity. The abs at 560 nm was decreased in K562 cancer cells treated with combination of 10 nM Pira and 10 or 100 μM GA, as it changed to 81 or 72% compared with the control group, respectively. The abs at 560 nm was significantly decreased in K562/Dox cancer cells treated with a combination of 10 nM Pira and 10 or 100 μM GA, as it changed to 72 or 70% compared with the control group, and to 82 or 80% compared with the 10 nM Pira alone group, respectively. |ΔΨml in (C) treated K562 and (D) treated K562/Dox cancer cells and non-treated cells. The |ΔΨml decreased, reflecting a decrease in the ΔΨm. The |ΔΨml of K562 cancer cells significantly decreased with the combination of 10 nM Pira and 10 or 100 μM GA, as the |ΔΨml changed to 83 or 82% compared with the control group, and changed to 87 or 86% compared with the 10 nM Pira alone group, respectively. The |ΔΨml of K562/Dox cancer cells significantly decreased with the combination of 10 nM Pira and 10 or 100 μM GA, as the |ΔΨml changed to 87 or 86% compared with the control group, and to 92 or 90% compared with the 10 nM Pira alone group, respectively. Percentage (%) of change of ATP levels in (E) treated K562 and (F) treated K562/Dox cancer cells and non-treated cells. The minus % change of ATP levels indicates the decreasing ATP. [a]P<0.05 compared with control and [b]P<0.05 compared with 10 nM Pira. Abs, absorbance intensity; Pira, pirarubicin; GA, gallic acid; ΔΨm, mitochondrial membrane potential; Dox, doxorubicin.

Effect of GA on RF values. The RF values were revealed to be decreased in K562/Dox cancer cells treated with 50, 100 and 200 μM GA compared with the non-treated control group (Fig. 4D). This result indicated that GA may reverse drug resistance in K562/Dox cancer cells.

Effect of GA on pH_i in K562 and K562/Dox cancer cells. Fig. 4E revealed the percentage (%) of change in pH_i values in GA-treated K562 and K562/Dox cancer cells and in the non-treated control group. The changes in the pH_i values in GA-treated K562/Dox cells were illustrated but no significant

Table II. Kinetics of Pira uptake into K562 and K562/Dox cancer cells after treatment with various GA concentrations.

	K562 cancer cells		K562/Dox cancer cells			
GA, μM	V_+, nM/sec	k_+ x10^{-12} l/cell.sec	V_+, nM/sec	k_+ x10^{-12} l/cell.sec	V_a, nM/sec	k_a x10^{-12} l/cell.sec
0	2.2±0.2	2.24±0.21	1.4±0.1	1.41±0.14	1.5±0.2	4.06±0.98
10	1.7±0.1	1.86±0.09	1.2±0.2	1.24±0.22	1.3±0.3	4.17±0.93
50	1.5±0.2[a]	1.47±0.20[a]	1.3±0.2	1.26±0.18	0.9±0.1	2.65±0.48
100	1.5±0.1[a]	1.48±0.06[a]	1.3±0.2	1.26±0.24	0.9±0.2	2.48±0.58
200	0.9±0.2[a]	0.94±0.02[a]	1.1±0.2	1.06±0.19	0.6±0.1	1.34±0.31

[a]P<0.05 compared with control. V_+, rate of Pira uptake into the cells [(dF/dt) x (C_T/F_0), where C_T is the total drug concentration added to the cells and F_0 the Pira fluorescence at time=0]; V_a, rate of P-glycoprotein-mediated active efflux of Pira (referred to P-glycoprotein function); k_+, passive influx coefficient; k_a, P-glycoprotein-mediated active efflux coefficient (referred to P-glycoprotein function); Pira, pirarubicin; GA, gallic acid; Dox, doxorubicin.

changes were observed when compared with the non-treated control group for all concentrations of GA.

Discussion

GA is a natural phenolic compound found in several fruits and medicinal plants. It has been reported to have several health-promoting effects such as an anti-inflammatory activity that involved MAPK and NF-κB signaling pathways (45). GA and its derivatives have exhibited potential anticancer activity *in vitro* and *in vivo* (46,47). The anticancer activity has been revealed in several types of cancer cells, including ovarian cancer cells and HCT-15 colon cancer cells (48-52). There is evidence suggesting that GA is able to induce apoptosis and cell death (50,51). In the present study, it was observed that GA inhibited the proliferation of K562 and K562/Dox cancer cells in a concentration and time-dependent manner. Moreover, the morphology of treated K562 and K562/Dox cancer cells displayed apoptotic characteristics, such as rough cells and shrinking cells. These findings were consistent with the findings of Subramanian *et al* (50). That study investigated the anticancer activity of GA on HCT-15 cancer cells. The authors determined that GA induced HCT-15 cancer cell death via apoptotic pathways and further revealed evidence of apoptosis based on images of cell morphology. The images revealed typical signs of apoptosis, such as membrane blebbing and shrinking cells (50). In addition, the present study found that GA disrupted the cellular energy status by decreasing mitochondrial activity, ΔΨm and ATP levels in both K562 and K562/Dox cancer cells. Hence, it was inferred that GA was able to induce apoptotic cell death in K562 and K562/Dox cancer cells.

In the present study, the question of whether GA (an antioxidant compound) can modify the cytotoxicity of Pira (a pro-oxidant compound) in cancer cells was raised. It was herein demonstrated that the GA/Pira combination exhibited higher antiproliferative activity compared with Pira alone in K562 and K562/Dox cancer cells. Hence, the mechanism of action of the GA/Pira combination was investigated in K562 and K562/Dox cancer cells. The results demonstrated that GA/Pira decreased mitochondrial activity, ΔΨm and ATP levels in both K562 and K562/Dox cancer cells. These biological effects of the combination were higher compared with those of Pira alone in both types of cancer cells. The findings of the present study indicated that the synergistic actions of the combination treatment could aggravate the disturbance of mitochondrial activity, ΔΨm and ATP levels. Therefore, it was inferred that GA was able to enhance Pira-induced K562 and K562/Dox cancer cell death through cellular energy status disruption.

GA and its derivative compounds did not only enhance the anticancer activity of Pira, but also enhanced the effects of other anticancer drugs on various cancer cells. Aborehab and Osama (31) studied the effect of GA on the anticancer effects of paclitaxel on HeLa cervical cancer cells. The authors found that the combination of GA and paclitaxel exerted cytotoxic effects and induced apoptosis. The combination treatment also increased the levels of P53 and caspase 3. The authors suggested that GA augmented the effects of paclitaxel on cervical cancer cells. Wang *et al* (53) studied the effect of GA on the anticancer activity of cisplatin in the H446 human small cell lung cancer cell line. The authors revealed that the combination of GA and cisplatin exerted cytotoxic effects and induced ROS generation and apoptosis. The combination treatment increased the levels of apoptosis regulators, such as Bax, Apaf-1 and P53, in H446 cells. The authors suggested that GA enhanced the anticancer activity of cisplatin in H446 cells. The authors proposed that the mechanism of GA enhancement was through a ROS-dependent mitochondrial apoptotic pathway. In addition, Rajagopalan *et al* (54) studied the effect of GA-derived compounds on the anticancer activity of 5-fuorouracil in the A431 human squamous carcinoma cell line. The authors found that the combination of GA derivatives and 5-fuorouracil exhibited higher cytotoxicity compared with 5-fuorouracil alone in A431 cancer cells. Therefore, it was deduced that GA could enhance the efficacy of anticancer drugs, including paclitaxel, cisplatin, 5-fuorouracil and Pira, to induce cancer cell death.

Of note, the present study demonstrated that GA was able to inhibit cell proliferation and induce cell energy status disruption in K562/Dox cancer cells. K562/Dox is an MDR leukemia cancer cell line, which is associated with the overexpression of P-glycoprotein in the cell membrane. P-glycoprotein is an ATP-dependent transmembrane transporter that transports

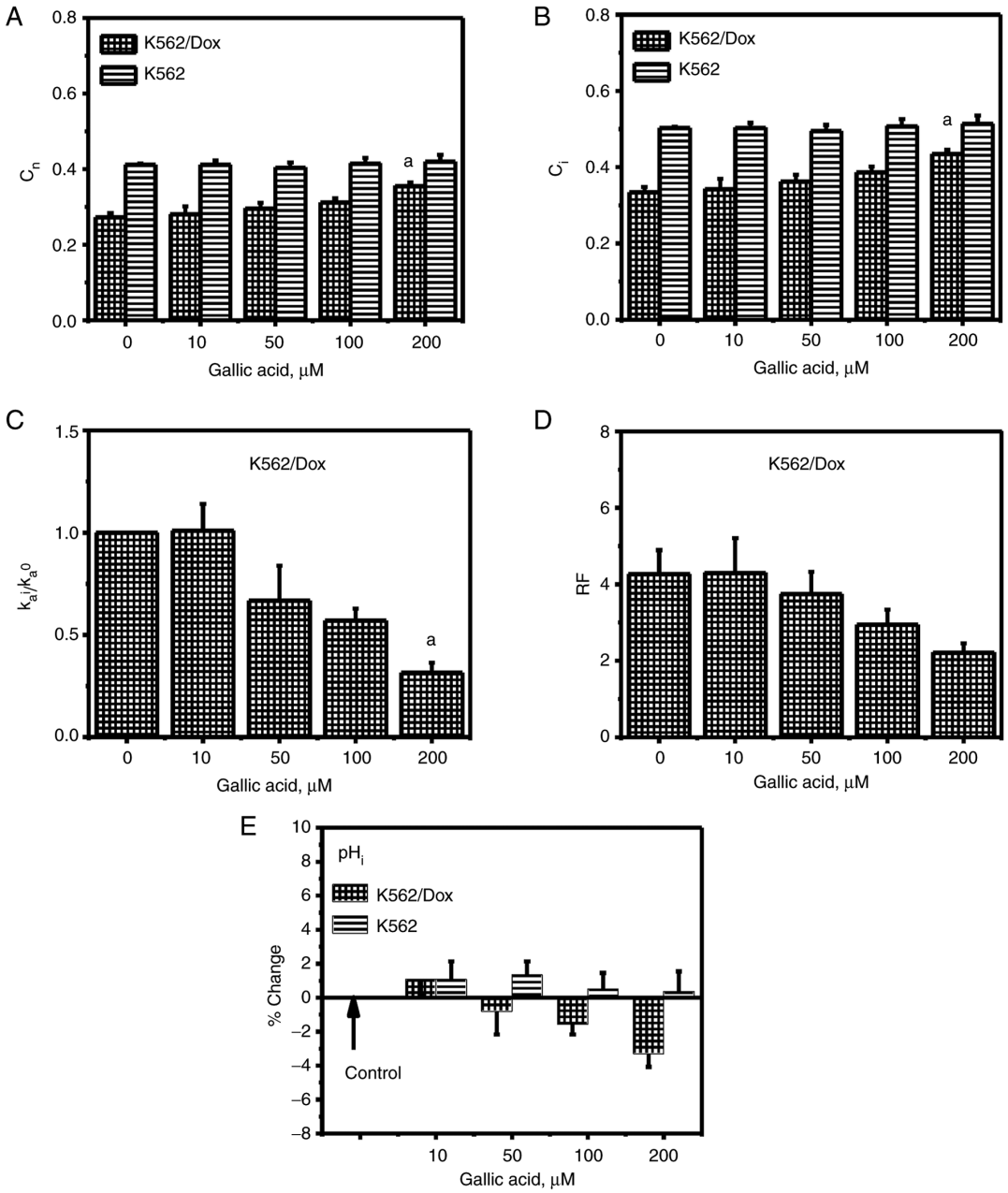

Figure 4. Pira accumulation and pHi in K562 and K562/Dox cancer cells. (A) C_n, (B) C_i and (C) k_a^i/k_a^0 ratio values in GA-treated K562 cells, GA-treated K562/Dox cancer cells and non-treated-cells. (D) RF values in GA-treated K562/Dox cancer cells. (E) Percentage (%) of change of pH_i values in GA-treated K562 and GA-treated-K562/Dox cancer cells and non-treated control group. [a]P<0.05 when compared with control. C_n, overall concentration of Pira accumulation in cells; C_i, concentration of Pira accumulation in cytoplasm; k_a^i/k_a^0, inhibition characterization of the P-glycoprotein-mediated efflux of Pira by GA; RF, resistance factor; Pira, pirarubicin; GA, gallic acid; Dox, doxorubicin; pH_i, intracellular pH.

drugs out of the cells, resulting in a decrease in intracellular drug concentration. A high P-glycoprotein function is commonly found in MDR cells (55,56). MDR poses a major challenge to leukemia chemotherapy. The present study found that GA was able to reverse drug resistance in K562/Dox cancer cells (low RF values). In addition, GA inhibited P-glycoprotein-mediated efflux of Pira in K562/Dox cancer cells (low k_a^i/k_a^0 values). This inhibitory effect led to an increase in the intracellular Pira concentration (high C_n and C_i values) in K562/Dox cancer cells. Hence, it was proposed that GA may reverse drug resistance in K562/Dox cancer cells by inhibiting the function of P-glycoprotein, resulting in increasing intracellular Pira accumulation that leads to K562/Dox cancer cell death. More importantly, it was demonstrated that the disruption of the cell energy status contributed to the reversal mechanisms of GA in K562/Dox cancer cells. The effect of verapamil on P-glycoprotein-mediated efflux of the Pira in K562/Dox was reported in a previous study by Mankhetkorn and Garnier-Suillerot (57). The authors reported that the verapamil concentrations required to obtain 50% inhibition of the P-glycoprotein-mediated efflux of the Pira (k_a^i/k_a^0 value=0.5) was 0.5±0.2 μM (57). To compare with GA in the present study, the effect of 50 and 100 μM GA was less than verapamil, whereas 200 μM GA was higher than verapamil. Of note, the results indicated that 10 μM GA did not affect k_a^i/k_a^0 whereas it still had an additive effect on cell survival. It was hypothesized that 10 μM GA may induce cell death via another

mechanism, not via inhibition of P-glycoprotein function. In addition, GA-derived compounds were reported to have the ability to modify P-glycoprotein function in KB-C2 cells (58).

The strength of the present study was that it investigated cancer cells that were alive and in an active state. Therefore, these results may be considered as highly representative of the behavior of cancer cells in cancerous diseases. In addition, the results revealed the mechanisms through which GA enhanced the anticancer effect of Pira on living MDR cancer cells.

The biological effects of the GA/Pira combination were more prominent compared with those of Pira alone in K562 and K562/Dox cancer cells. The efficacy of this combination depended on the concentration of GA. In addition, these findings indicated that GA was able to reverse drug resistance in living K562/Dox cancer cells by inhibiting the function of P-glycoprotein, resulting in increased intracellular Pira accumulation. More importantly, it was demonstrated that the cellular energy status disruption contributed to the reversal mechanisms of GA in K562/Dox cancer cells. Finally, it was determined that GA enhanced the Pira-induced anticancer effects on living K562 and K562/Dox cancer cells through cellular energy status impairment and by inhibiting the function of P-glycoprotein. However, the anticancer properties of the GA/Pira combination require further evaluation in *in vivo* studies.

Acknowledgements

KTNA would like to thank the Ph.D. degree program in Biomedical Sciences, Faculty of Associated Medical Sciences, Chiang Mai University, under the CMU Presidential Scholarship (Chiang Mai, Thailand). The authors would like to thank the Department of Radiologic Technology, Faculty of Associated Medical Sciences, Chiang Mai University for their support (Chiang Mai, Thailand).

Funding

The present study was supported by the Ph.D. degree program in Biomedical Sciences, Faculty of Associated Medical Sciences, Chiang Mai University, under the CMU Presidential Scholarship. The present study was also partially supported by Chiang Mai University and Faculty of Associated Medical Sciences, Chiang Mai University.

Availability of data and materials

The datasets used and/or analyzed during the present study are available from the corresponding author on reasonable request.

Authors' contributions

KTA performed the acquisition, analysis and interpretation of data and drafted the manuscript. SW and BS performed acquisition and analysis of data. SK, CU, ST and JP performed interpretation of data and drafted the manuscript, revising it critically for important intellectual content. MT conceived and designed the study, as well as performed acquisition, analysis and interpretation of data, drafted the manuscript, revising it critically for important intellectual content, and provided final approval of the version to be published. All authors read and approved the final manuscript.

Ethics approval and consent to participate

Not applicable.

Patient consent for publication

Not applicable.

Competing interests

The authors declare that they have no competing interests.

References

1. Bray F, Ferlay J, Soerjomataram I, Siegel RL, Torre LA and Jemal A: Global cancer statistics 2018: GLOBOCAN estimates of incidence and mortality worldwide for 36 cancers in 185 countries. CA Cancer J Clin 68: 394-424, 2018.
2. Gewirtz DA: A critical evaluation of the mechanisms of action proposed for the antitumor effects of the anthracycline antibiotics adriamycin and daunorubicin. Biochem Pharmacol 57: 727-741, 1999.
3. Minotti G, Menna P, Salvatorelli E, Cairo G and Gianni L: Anthracyclines: Molecular advances and pharmacologic developments in antitumor activity and cardiotoxicity. Pharmacol Rev 56: 185-229, 2004.
4. Meredith AM and Dass CR: Increasing role of the cancer chemotherapeutic doxorubicin in cellular metabolism. J Pharm Pharmacol 68: 729-741, 2016.
5. Miller AA and Salewski E: Prospects for pirarubicin. Med Pediatr Oncol 22: 261-268, 1994.
6. Tsuruo T, Iida H, Tsukagoshi S and Sakurai Y: 4'-O-tetrahydropyranyladriamycin as a potential new antitumor agent. Cancer Res 42: 1462-1467, 1982.
7. Kunimoto S, Miura K, Takahashi Y, Takeuchi T and Umezawa H: Rapid uptake by cultured tumor cells and intracellular behavior of 4'-O-tetrahydropyranyladriamycin. J Antibiot (Tokyo) 36: 312-317, 1983.
8. Mizutani H, Hotta S, Nishimoto A, Ikemura K, Miyazawa D, Ikeda Y, Maeda T, Yoshikawa M, Hiraku Y and Kawanishi S: Pirarubicin, an anthracycline anticancer agent, induces apoptosis through generation of hydrogen peroxide. Anticancer Res 37: 6063-6069, 2017.
9. Michieli M, Damiani D, Michelutti A, Candoni A, Masolini P, Scaggiante B, Quadrifoglio F and Baccarani M: Restoring uptake and retention of daunorubicin and idarubicin in P170-related multidrug resistance cells by low concentration D-verapamil, cyclosporin-A and SDZ PSC 833. Haematologica 79: 500-507, 1994.
10. Xia Q, Wang ZY, Li HQ, Diao YT, Li XL, Cui J, Chen XL and Li H: Reversion of p-glycoprotein-mediated multidrug resistance in human leukemic cell line by diallyl trisulfide. Evid Based Complement Alternat Med 2012: 719805, 2012.
11. Barrand MA, Bagrij T and Neo SY: Multidrug resistance-associated protein: A protein distinct from P-glycoprotein involved in cytotoxic drug expulsion. Gen Pharmacol 28: 639-645, 1997.
12. Choi CH: ABC transporters as multidrug resistance mechanisms and the development of chemosensitizers for their reversal. Cancer Cell Int 5: 30, 2005.
13. Yang K, Wu J and Li X: Recent advances in the research of P-glycoprotein inhibitors. Biosci Trends 2: 137-146, 2008.
14. Inaba M, Fujikura R, Tsukagoshi S and Sakurai Y: Restored in vitro sensitivity of adriamycin- and vincristine-resistant P388 leukemia with reserpine. Biochem Pharmacol 30: 2191-2194, 1981.
15. Mocanu MM, Nagy P and Szöllősi J: Chemoprevention of breast cancer by dietary polyphenols. Molecules 20: 22578-22620, 2015.
16. Punia R, Raina K, Agarwal R and Singh RP: Acacetin enhances the therapeutic efficacy of doxorubicin in non-small-cell lung carcinoma cells. PLoS One 12: e0182870, 2017.

17. Liu R, Ji P, Liu B, Qiao H, Wang X, Zhou L, Deng T and Ba Y: Apigenin enhances the cisplatin cytotoxic effect through p53-modulated apoptosis. Oncol Lett 13: 1024-1030, 2017.
18. Bansal T, Jaggi M, Khar RK and Talegaonkar S: Emerging significance of flavonoids as P-glycoprotein inhibitors in cancer chemotherapy. J Pharm Pharm Sci 12: 46-78, 2009.
19. Naus PJ, Henson R, Bleeker G, Wehbe H, Meng F and Patel T: Tannic acid synergizes the cytotoxicity of chemotherapeutic drugs in human cholangiocarcinoma by modulating drug efflux pathways. J Hepatol 46: 222-229, 2007.
20. Muhammad N, Steele R, Isbell TS, Philips N and Ray RB: Bitter melon extract inhibits breast cancer growth in preclinical model by inducing autophagic cell death. Oncotarget 8: 66226-66236, 2017.
21. Haslam E and Cai Y: Plant polyphenols (vegetable tannins): Gallic acid metabolism. Nat Prod Rep 11: 41-66, 1994.
22. Zhao B and Hu M: Gallic acid reduces cell viability, proliferation, invasion and angiogenesis in human cervical cancer cells. Oncol Lett 6: 1749-1755, 2013.
23. Locatelli C, Filippin-Monteiro FB and Creczynski-Pasa TB: Alkyl esters of gallic acid as anticancer agents: A review. Eur J Med Chem 60: 233-239, 2013.
24. Priscilla DH and Prince PS: Cardioprotective effect of gallic acid on cardiac troponin-T, cardiac marker enzymes, lipid peroxidation products and antioxidants in experimentally induced myocardial infarction in Wistar rats. Chem Biol Interact 179: 118-124, 2009.
25. Lu Z, Nie G, Belton PS, Tang H and Zhao B: Structure-activity relationship analysis of antioxidant ability and neuroprotective effect of gallic acid derivatives. Neurochem Int 48: 263-274, 2006.
26. Omóbòwálé TO, Oyagbemi AA, Folasire AM, Ajibade TO, Asenuga ER, Adejumobi OA, Ola-Davies OE, Oyetola O, James G, Adedapo AA and Yakubu MA: Ameliorative effect of gallic acid on doxorubicin-induced cardiac dysfunction in rats. J Basic Clin Physiol Pharmacol 29: 19-27, 2018.
27. Kim SH, Jun CD, Suk K, Choi BJ, Lim H, Park S, Lee SH, Shin HY, Kim DK and Shin TY: Gallic acid inhibits histamine release and pro-inflammatory cytokine production in mast cells. Toxicol Sci 91: 123-131, 2006.
28. Punithavathi VR, Prince PS, Kumar R and Selvakumari J: Antihyperglycaemic, antilipid peroxidative and antioxidant effects of gallic acid on streptozotocin induced diabetic Wistar rats. Eur J Pharmacol 650: 465-471, 2011.
29. Oyagbemi AA, Omobowale TO, Saba AB, Olowu ER, Dada RO and Akinrinde AS: Gallic acid ameliorates cyclophosphamide-induced neurotoxicity in wistar rats through free radical scavenging activity and improvement in antioxidant defense system. J Diet Suppl 13: 402-419, 2016.
30. Supawat B, Moungthong P, Chanloi C, Jindachai N, Tima S, Kothan S, Udomtanakunchai C and Tungjai M: Effects of gadolinium-based magnetic resonance imaging contrast media on red blood cells and K562 cancer cells. J Trace Elem Med Biol 62: 126640, 2020.
31. Aborehab NM and Osama N: Effect of Gallic acid in potentiating chemotherapeutic effect of Paclitaxel in HeLa cervical cancer cells. Cancer Cell Int 19: 154, 2019.
32. Gu R, Zhang M, Meng H, Xu D and Xie Y: Gallic acid targets acute myeloid leukemia via Akt/mTOR-dependent mitochondrial respiration inhibition. Biomed Pharmacother 105: 491-497, 2018.
33. Liao CC, Chen SC, Huang HP and Wang CJ: Gallic acid inhibits bladder cancer cell proliferation and migration via regulating fatty acid synthase (FAS). J Food Drug Anal 26: 620-627, 2018.
34. Liu Z, Li D, Yu L and Niu F: Gallic acid as a cancer-selective agent induces apoptosis in pancreatic cancer cells. Chemotherapy 58: 185-194, 2012.
35. Tang HM and Cheung PCK: Gallic acid triggers iron-dependent cell death with apoptotic, ferroptotic, and necroptotic features. Toxins (Basel) 11: 492, 2019.
36. Wang K, Zhu X, Zhang K, Zhu L and Zhou F: Investigation of gallic acid induced anticancer effect in human breast carcinoma MCF-7 cells. J Biochem Mol Toxicol 28: 387-393, 2014.
37. Weng SW, Hsu SC, Liu HC, Ji BC, Lien JC, Yu FS, Liu KC, Lai KC, Lin JP and Chung JG: Gallic acid induces DNA damage and inhibits DNA repair-associated protein expression in human oral cancer SCC-4 cells. Anticancer Res 35: 2077-2084, 2015.
38. Kothan S, Dechsupa S, Leger G, Moretti JL, Vergote J and Mankhetkorn S: Spontaneous mitochondrial membrane potential change during apoptotic induction by quercetin in K562 and K562/adr cells. Can J Physiol Pharmacol 82: 1084-1090, 2004.
39. Tungjai M, Phathakanon N and Rithidech KN: Effects of medical diagnostic Low-dose X rays on human lymphocytes: Mitochondrial membrane potential, apoptosis and cell cycle. Health Phys 112: 458-464, 2017.
40. Supawat B, Udomtanakunchai C, Kothan S and Tungjai M: The effects of iodinated radiographic contrast media on multidrug-resistant K562/Dox cells: Mitochondria impairment and P-glycoprotein inhibition. Cell Biochem Biophys 77: 157-163, 2019.
41. Yang NC, Ho WM, Chen YH and Hu ML: A convenient one-step extraction of cellular ATP using boiling water for the luciferin-luciferase assay of ATP. Anal Biochem 306: 323-327, 2002.
42. Reungpatthanaphong P and Mankhetkorn S: Modulation of multidrug resistance by artemisinin, artesunate and dihydroartemisinin in K562/adr and GLC4/adr resistant cell lines. Biol Pharm Bull 25: 1555-1561, 2002.
43. Garnier-Suillerot A, Marbeuf-Gueye C, Salerno M, Loetchutinat C, Fokt I, Krawczyk M, Kowalczyk T and Priebe W: Analysis of drug transport kinetics in multidrug-resistant cells: Implications for drug action. Curr Med Chem 8: 51-64, 2001.
44. Frézard F, Pereira-Maia E, Quidu P, Priebe W and Garnier-Suillerot A: P-glycoprotein preferentially effluxes anthracyclines containing free basic versus charged amine. Eur J Biochem 268: 1561-1567, 2001.
45. Bai J, Zhang Y, Tang C, Hou Y, Ai X, Chen X, Zhang Y, Wang X and Meng X: Gallic acid: Pharmacological activities and molecular mechanisms involved in inflammation-related diseases. Biomed Pharmacother 133: 110985, 2021.
46. Bhattacharya S, Muhammad N, Steele R, Peng G and Ray RB: Immunomodulatory role of bitter melon extract in inhibition of head and neck squamous cell carcinoma growth. Oncotarget 7: 33202-33209, 2016.
47. Sun J, Chu YF, Wu X and Liu RH: Antioxidant and antiproliferative activities of common fruits. J Agric Food Chem 50: 7449-7454, 2002.
48. Dai J and Mumper RJ: Plant phenolics: Extraction, analysis and their antioxidant and anticancer properties. Molecules 15: 7313-7352, 2010.
49. De A, De A, Papasian C, Hentges S, Banerjee S, Haque I and Banerjee SK: Emblica officinalis extract induces autophagy and inhibits human ovarian cancer cell proliferation, angiogenesis, growth of mouse xenograft tumors. PLoS One 8: e72748, 2013.
50. Subramanian AP, Jaganathan SK, Mandal M, Supriyanto E and Muhamad II: Gallic acid induced apoptotic events in HCT-15 colon cancer cells. World J Gastroenterol 22: 3952-3961, 2016.
51. Sourani ZM, Pourgheysari BP, Beshkar PM, Shirzad HP and Shirzad MM: Gallic acid inhibits proliferation and induces apoptosis in lymphoblastic leukemia cell line (C121). Iran J Med Sci 41: 525-530, 2016.
52. Yoshino M, Haneda M, Naruse M, Htay HH, Iwata S, Tsubouchi R and Murakami K: Prooxidant action of gallic acid compounds: Copper-dependent strand breaks and the formation of 8-hydroxy-2'-deoxyguanosine in DNA. Toxicol In Vitro 16: 705-709, 2002.
53. Wang R, Ma L, Weng D, Yao J, Liu X and Jin F: Gallic acid induces apoptosis and enhances the anticancer effects of cisplatin in human small cell lung cancer H446 cell line via the ROS-dependent mitochondrial apoptotic pathway. Oncol Rep 35: 3075-3083, 2016.
54. Rajagopalan R, Jain SK and Trivedi P: Synergistic anti-cancer activity of combined 5-fuorouracil and gallic acid-stearylamine conjugate in a431 human squamous carcinoma cell line. Trop J Pharm Res 18: 471-477, 2019.
55. Gillet JP, Efferth T and Remacle J: Chemotherapy-induced resistance by ATP-binding cassette transporter genes. Biochim Biophys Acta 1775: 237-262, 2007.
56. Mimeault M, Hauke R and Batra SK: Recent advances on the molecular mechanisms involved in the drug resistance of cancer cells and novel targeting therapies. Clin Pharmacol Ther 83: 673-691, 2008.
57. Mankhetkorn S and Garnier-Suillerot A: The ability of verapamil to restore intracellular accumulation of anthracyclines in multidrug resistant cells depends on the kinetics of their uptake. Eur J Pharmacol 343: 313-321, 1998.
58. Kitagawa S, Nabekura T, Kamiyama S, Takahashi T, Nakamura Y, Kashiwada Y and Ikeshiro Y: Effects of alkyl gallates on P-glycoprotein function. Biochem Pharmacol 70: 1262-1266, 2005.